Nanoscale Res Lett (2009) 4:234–239
DOI 10.1007/s11671-008-9231-4

NANO EXPRESS

Effects of Gas Composition on Highly Efficient Surface Modification of Multi-Walled Carbon Nanotubes by Cation Treatment

Wen-Shou Tseng · Chyuan-Yow Tseng · Cheng-Tzu Kuo

Received: 24 October 2008 / Accepted: 2 December 2008 / Published online: 16 December 2008

Abstract High incident energy hydrogen and/or oxygen cations are generated by electron cyclotron resonance system, and then used to highly efficiently modify multi-walled carbon nanotubes (MWCNTs). The effects of various H_2/O_2 gas compositions on the modification process are studied. A systematic characterization method utilizing a combination of X-ray photoelectron spectroscopy (XPS), scanning electron microscopy, Raman spectroscopy, and thermogravimetric analysis (TGA) is used to evaluate the effects of various H_2/O_2 gas compositions on MWCNT functionalization. The Raman results show that the I_D/I_G ratio is directly affected by H_2 concentration in gas mixture, and the treatment applying a H_2/O_2 gas mixture with ratio of 40/10 (sccm/sccm) can yield the nanotubes with the highest I_D/I_G ratio (1.27). The XPS results suggest that the gas mixture with ratio of 25/25 (sccm/sccm) is most effective in introducing oxygen-containing functional groups and reducing amorphous carbon. The TGA suggests that the structural change of the treated nanotubes is marginal by this method with any gas condition.

Keywords Multi-walled carbon nanotubes · Electron cyclotron resonance plasma · X-ray photoelectron spectroscopy · Functionalization · Raman spectroscopy

W.-S. Tseng
Department of Materials Science and Engineering, National Chiao Tung University, HsinChu, Taiwan

C.-Y. Tseng
Department of Vehicle Engineering, National Pingtung University of Science and Technology, Neipu, Pingtung, Taiwan

C.-T. Kuo (✉)
Institute of Materials and Systems Engineering, MingDao University, ChangHua, Taiwan
e-mail: marine.mse92g@g2.nctu.edu.tw

Introduction

Recently, nanostructured materials have attracted intensive attention in many applications because of their unique properties [1–4]. As one of the most promising materials, and to make the best use of their singular properties, carbon nanotubes (CNTs) can be modified or prepared by different processes to meet the requirements of specifically potential applications [5–7]. The process of facially modifying the nanotubes through changing their surface structure is a relatively simple technique and has been widely investigated [8–10]. The main premise behind these methods is to affix highly polar functional groups to the surface of the nanotubes to enhance their polarity so as to disperse them in the aqueous or polymer matrix. Currently, acid treatment is the most commonly used technique for this process. However, it is mentioned that the use of harsh acids would give rise to issues concerning the drastic changes of the structural integrity, length, and even useful properties of the nanotubes [11–15].

Recently, plasma treatment has been proven to be an attractive alternative and has become increasingly popular in the functionalization of CNTs because the procedure is solvent-free, time-efficient, versatile, and environmental friendly [16–23]. To date, many approaches have been investigated to demonstrate the viability and performance of plasma treatment for surface functionalization of CNTs. In these studies, various gases, such as N_2 [17], H_2 [18], O_2 [19–21], NH_3 [16, 19, 20], and CF_4 [19, 23] have been used. Generally, the plasma is generated using glow discharge, radio frequency discharge, or microwave discharge

at low-vacuum pressure. The high-energy particles generated in the plasma can then satisfy the chemical bonding energies on the surface of the tubes thereby initiating chemical reactions. In addition, their density and energy can be readily regulated by external parameters, such as the electromagnetic frequency, power, and gas pressure, to achieve optimum conditions for the required production scale and efficiency [16]. However, some studies mention that the nanotubes could be overheated by hyperthermal plasma [19, 21].

In our previous study, through using H_2/O_2 gas mixture as etching gas, electron cyclotron resonance (ECR) plasma treatment was shown effective to functionalize multi-walled carbon nanotubes (MWCNTs) with minor negative consequences in nanotube structure [24]. In the process, high incident energy hydrogen and oxygen cations generated and extracted by ECR plasma system were used to create free radical defects on the surface of the MWCNTs through ion bombardment; oxygen cations with the high reduction potential present in the ion stream were simultaneously involved in initiating covalent bonding reactions on the surface of the tubes. The ratio of H_2 to O_2 is critical to the process because it directly correlates with the composition of the generated cations. In this study, the effect of gas composition on the functionalization process is investigated, by providing various H_2/O_2 gas mixtures to the treatment through the control of gas flow ratio. Furthermore, the manner in which the gas conditions correlate with morphology and structural changes of the nanotubes will be studied through the use of some advanced instruments.

Experimental

Samples of pristine MWCNTs weighing 0.05 g sourced from a commercial organization were loaded into the stainless steel crucible and placed on the process stage of the ECR plasma system as shown in Fig. 1. Chamber pressure was maintained at 4.2×10^{-3} Torr. The 2.45 GHz microwave with output power of approximately 750 W was inserted into the plasma chamber through a quartz window. H_2 and/or O_2 gas mixtures were fed as etching gases with controlled gas flow ratios of 50/0, 40/10, 25/25, 10/40, and 0/50 (H_2/O_2 (sccm/sccm)), which are equivalent to H_2 concentrations of 100, 80, 50, 20, and 0 vol.%, respectively. A bias voltage of −250 V was applied to the process stage. When the stage temperature reached 400 °C, each sample was treated for 5 min. The ionic current was monitored using a current ammeter connected to the process stage.

In order to evaluate the surface morphology and structural changes, the samples were dispersed on a silicon wafer using ethanol and measured using scanning electron microscopy

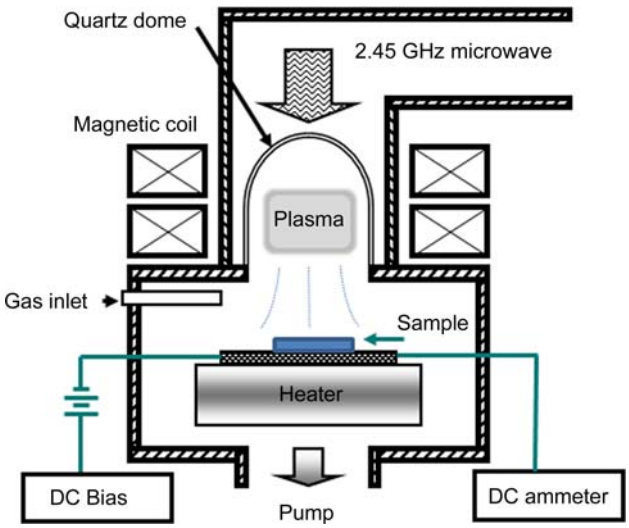

Fig. 1 Schematic of the ECR plasma apparatus

(SEM) (JEOL, JSM-6500F). The microstructure of the pristine sample was characterized by transmission electron microscopy (TEM) (JEOL, JEM-2100) through dispersing sample powders on Lacey carbon grids using ethanol. X-ray photoelectron spectroscopy (XPS) was performed to determine the chemical changes at the surface of the nanotubes. Thermogravimetric analysis (TGA) (TA-500) was applied to investigate the changes in thermal stability with a heating rate of 10 °C/min and an air flow of 60 mL/min. Raman spectroscopy (Jobin YVON LabRam HR800) was used to evaluate structural defects in the CNTs.

Results and Discussion

As shown in Fig. 2, the SEM (Fig. 2a) and TEM (Fig. 2b) images show that the pristine MWCNTs are highly tangled with diameters ranging from 15 to 40 nm. The TEM image (Fig. 2b) also shows that the nanotubes are with densely distributed defects. After the ECR plasma treatment with a H_2/O_2 ratio of 40/10 (sccm/sccm), as depicted in Fig. 2c, d, the morphologies, structural and the diameter distributions of the sample do not show any observable difference in comparison with those of the pristine sample. In contrast to Fig. 2b, the TEM image in Fig. 2d shows that the dispersion ability of the nanotubes is increased after the plasma treatment so that the nanotube bundle can be significantly separated. Meanwhile, the insignificant change in morphology and structure can also be observed when sample is treated with any gas condition.

Figure 3 shows the XPS survey spectra of the untreated and the ECR-plasma-treated MWCNTs. It is noted that the spectra showing the presence of carbon and oxygen on the treated and untreated samples are normalized with respect

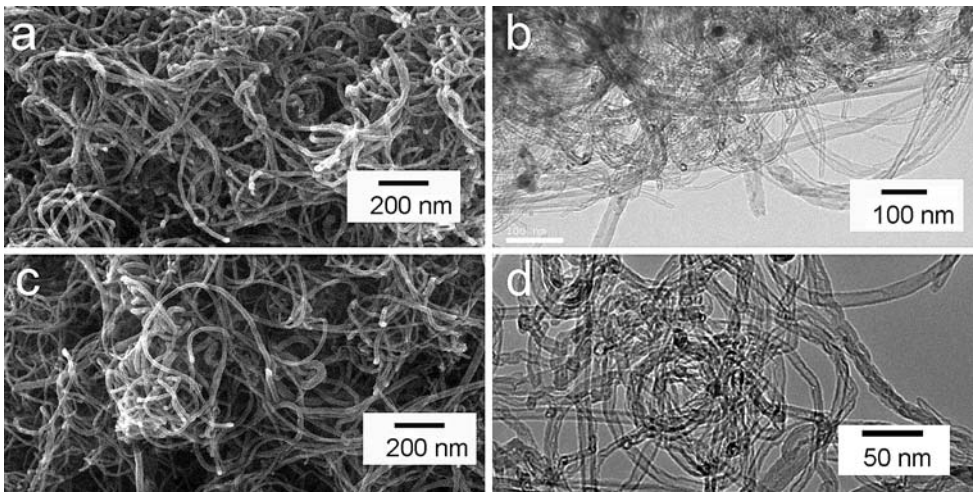

Fig. 2 **a** SEM and **b** TEM images of the pristine MWCNTs, **c** SEM, and **d** TEM images of ECR-plasma-treated MWCNTs with 5 min exposure under H_2/O_2 gas compositions of 40/10 (sccm/sccm)

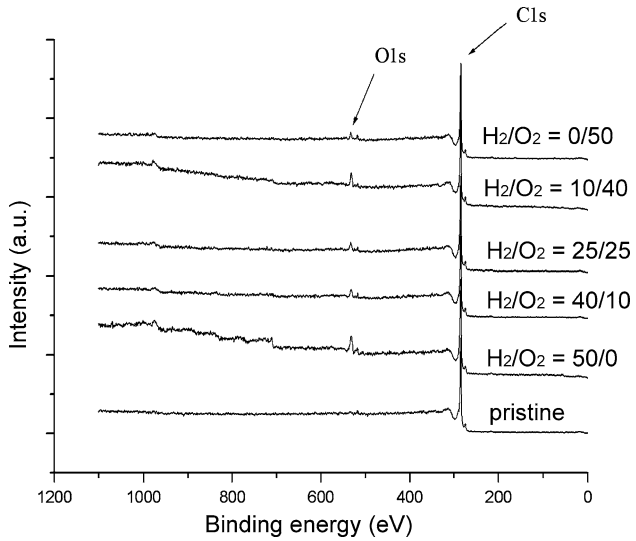

Fig. 3 XPS survey spectra of the pristine MWCNTs and the ECR-plasma-treated MWCNTs under various H_2/O_2 (sccm/sccm) gas compositions

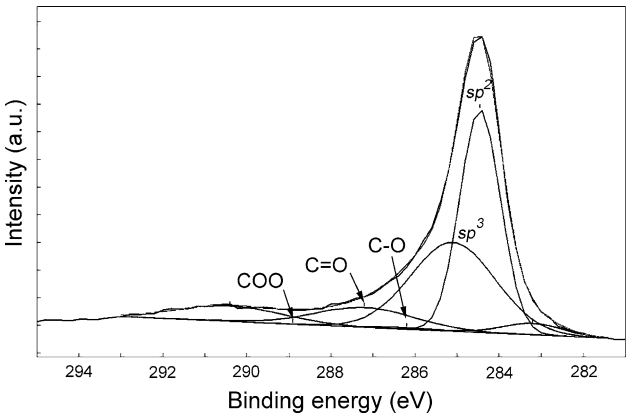

Fig. 4 XPS C 1s spectra of the pristine MWCNTs and the five chemical species: (1) graphite; (2) sp^3 carbons; (3) hydroxyl groups; (4) carbonyl groups; and (5) carboxyl groups

to C 1s intensity for comparison purposes. In contrast to the spectrum of the pristine MWCNTs, a higher concentration of oxygen is introduced to the surface of the nanotubes treated by the ECR plasma using any gas composition.

As a reference spectrum, the XPS C 1s spectrum of the pristine MWCNTs was recorded and is shown in Fig. 4. Based on the previous studies [19, 25], the spectra are deconvoluted into five Gaussian peaks centered at 284.5, 285.1, 286.2, 287.2, and 288.9 eV. Here, the main peak at 284.5 eV originates from a graphite signal. The peak at 285.1 eV is attributed to sp^3 carbon [19–21, 25]. The peaks at 286.2, 287.2, and 288.9 eV correspond to hydroxyl, carbonyl (or ether), and carboxyl (or ester) groups, respectively. A peak attributed to π–π^* shake-up bonds is observed at 290.4 eV [20, 26]; and the peak at 283.2 eV originates from carbidic carbon [27]. Meanwhile, the deconvolution results also show that the oxygen functional groups have been grafted onto the surface of the pristine MWCNTs with a concentration of approximately 11.2%. This is consistent with the description provided by the vendor that the raw materials were treated using mild acids prior to shipment. Furthermore, the results show that the MWCNTs are still composed of approximately 40% amorphous carbon.

For a detailed comparison, all C 1s spectra of the MWCNT samples are presented in Fig. 5 and the calculated results are summarized in Table 1. Note that the [O]/[C] ratio given in Table 1 is based on the relative percentage of three carboxyl groups to the total number of carbon atoms detected. As shown in Fig. 5 and Table 1, after the samples are treated by the plasma treatment, the XPS measurements show that the concentrations of the graphite, sp^3 carbons, and oxygen-containing functional groups are different according to the gas mixture composition. Also, it is clear that when the samples of the MWCNTs are treated with a H_2/O_2 ratio of 25/25 (sccm/sccm), the highest concentration of

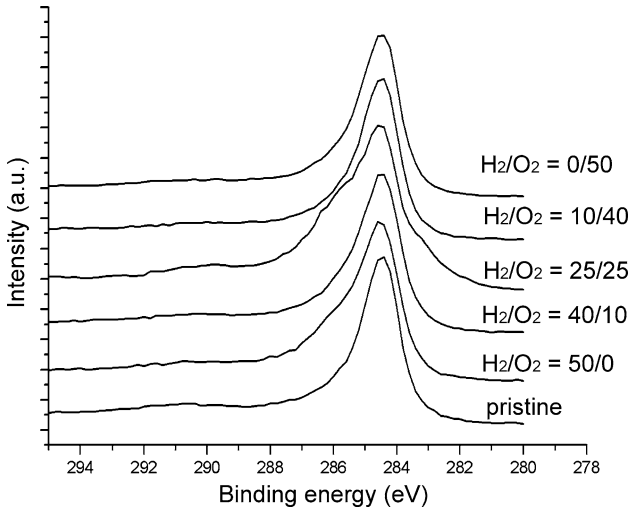

Fig. 5 XPS C 1s spectra of the pristine MWCNTs and the ECR-plasma-treated MWCNTs after 5 min of exposure under various H_2/O_2 (sccm/sccm) gas compositions

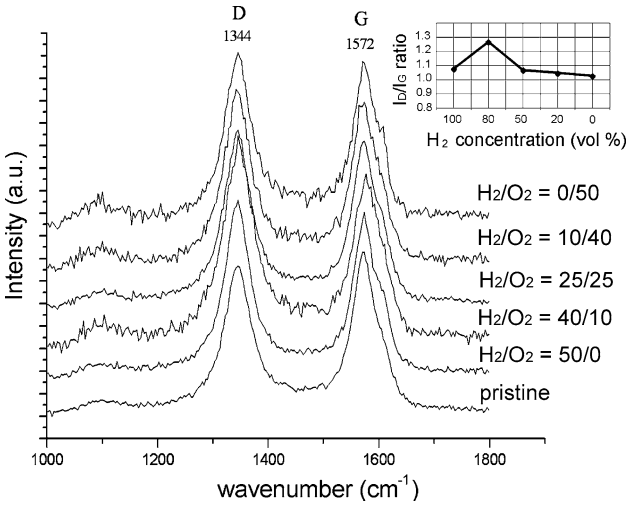

Fig. 6 Raman spectra of the pristine MWCNTs and the ECR-plasma-treated MWCNTs after 5 min of exposure under various H_2/O_2 (sccm/sccm) gas conditions

oxygenated functional groups is achieved whilst the concentration of amorphous carbon is minimized.

Note that the amount of surface defects is important for functional groups to form on the nanotube surface [10]. In order to evaluate the formation of defects on the nanotube surface by the ECR plasma treatment using different gas compositions, the Raman spectra of the pristine and the plasma-treated MWCNTs are presented in Fig. 6. Two characteristic peaks are observed and attributed to the D and G bands. The spectra have been normalized with respect to the G band for comparison. The intensity of the D band, at frequencies around 1,344 cm^{-1}, is correlated with structural disorder of CNTs, which originates from the defects including disordered materials, poor graphitization, functionalized carbon, and the amorphous carbon on the sidewall of nanotubes [28–30]. The G band at frequencies around 1,572 cm^{-1} is activated by the graphite signal [30]. It is suggested that the I_D/I_G ratio is closely associated with the defect density on the walls of the MWCNTs [30]. Therefore, the intensity ratio can be used to evaluate the formation of defects which are preferential sites for functionalization.

As expected, all I_D/I_G ratios are increased after plasma treatment with any gas composition. As shown in the inset of Fig. 6, the I_D/I_G ratio increases from 1.03 to 1.27 when the H_2 concentration increases from 0 to 80 vol.%. Note that the ion density is very important for surface etching. By comparing the ionic current, it is found that current increases from 0.12 to 0.47 A while the H_2 concentration increases from 0 to 100%. This shows that the ion density of the cation stream increases as H_2 concentration increases. This leads to higher I_D/I_G ratio when H_2 concentration of the etching gas is higher. However, it is also shown that the ratio decreases to 1.08 when the nanotubes are treated with pure H_2 gas (H_2/O_2 of 50/0 (sccm/sccm)). This could be because the ion bombardment under this gas condition can heavily etch the surface of the nanotubes to the extent that the concentration of amorphous carbon coated on the

Table 1 The MWCNT specimen treated under various H_2/O_2 gas compositions; the characterization results of XPS; and the I_D/I_G ratio of Raman spectra

Specimen (H_2/O_2 (sccm/sccm))	XPS						Raman
	sp^2 (%)	sp^3 (%)	–C–O (%)	–C=O (%)	–COO (%)	[O]/[C][a] (%)	(I_D/I_G)
0/50	44.2	44.6	<0.1	9.4	1.7	11.1	1.03
10/40	40.5	39.5	11.9	0.8	7.3	20	1.05
25/25	42.8	26.1	13.8	17.3	<0.1	31.1	1.07
40/10	36.8	49.1	0.6	0.5	12.9	14	1.27
50/0	30.8	54	2.1	11	2.2	15.3	1.08
Pristine	48.8	40	1	8.4	1.8	11.2	0.89

[a] [O]/[C]: the ratio of oxygenated groups to the total number of carbon atoms detected

surface could thus be raised from 40 to 54% as shown in Table 1. The thick amorphous carbon can prevent defects from further forming on the surface during ion bombardment so that the I_D/I_G ratio is significantly smaller than that of the nanotubes treated with the etching gas containing 20 vol.% oxygen ($I_D/I_G = 1.27$, H_2/O_2 of 40/10 (sccm/sccm)). Apart from their involvement in ion bombardment, the generated oxygen cations can also act as highly reactive chemical species which form covalent bonds with the amorphous carbon and then nanotube surface. More specifically, the amorphous carbon layer is more reactive than the cylindrical walls to form volatile products with the oxygen cations. The products are then pumped out by the vacuum system. Thus, as shown in Table 1, treatment using a H_2/O_2 mixture can increase the concentration of oxygenated functional groups whilst also reducing the concentration of amorphous carbon. On the other hand, treatment with pure O_2 gas (with the exception of increasing the I_D/I_G ratio) does not yield any other obvious effects in regard to the purity of CNTs and the concentration of functional groups when compared with the pristine MWCNTs. This indicates that a H_2/O_2 mixture not only facilitates defect formation but also promotes covalent bonding in this case. Therefore, even with the addition of 20 vol.% H_2 (H_2/O_2 of 10/40 (sccm/sccm)) in gas, there is still a significant removal of amorphous carbon and formation of oxygen-containing groups on the nanotube surface.

Figure 7 shows the weight-derivative curves of TGA analysis on the pristine MWCNT samples and the ECR-plasma-treated MWCNTs. The results show that with a decomposition temperature of 600 °C, the pristine MWCNT samples are the most thermally stable with respect to oxidative degradation. Correspondingly, the MWCNTs treated by the ECR plasma with a gas composition of 40/10 (sccm/sccm) have the lowest decomposition temperature (594 °C). It should be noted that the oxidation stability is a function of the combined effect of defects and the diameter of the nanotubes [12, 31, 32]. With the same diameter distribution, the results are in agreement with the hypothesis that the decrease of the oxidation reaction temperature is mainly a result of the defects produced by the plasma treatment. The marginal differences between untreated and treated samples reflect the fact that the effect of gas composition on structural integrity of the nanotubes is insignificant in this case.

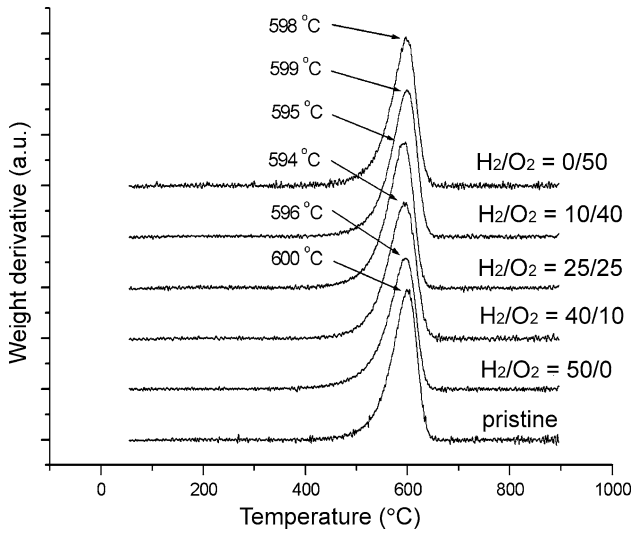

Fig. 7 Weight-derivative curves of TGA on the pristine MWCNTs and the ECR-plasma-treated MWCNTs under various H_2/O_2 (sccm/sccm) gas compositions

Conclusions

In this article, the effects of various H_2/O_2 gas compositions on the functionalization of MWCNTs using ECR plasma system are studied. The results of Raman spectroscopy show that the cation treatment is effective in introducing defects to the nanotube surface; and this is affected by H_2 concentration in gas mixture provided. Meanwhile, with a H_2/O_2 mixture of 40/10 (sccm/sccm), the treatment can produce nanotubes with highest I_D/I_G ratio (1.27). As demonstrated by the characterization results of XPS, the gas composition strongly correlates with the functionalization extent and amorphous carbon removal. As compared to the other gas composition applied in this study, the treatment using a H_2/O_2 mixture of 25/25 (sccm/sccm) is found to be the most effective gas mixture to graft oxygen-containing functional groups and remove the amorphous carbon on the surface of the nanotubes. Specifically, by using this gas condition to conduct the plasma treatment, the highest concentration of 31.1% (after 5 min exposure) of oxygenated functional groups on the surface of CNTs is achieved. In addition, the amorphous carbon can also be significantly removed. On the other hand, the results also indicate that the structural and morphological changes, if any, are marginally effected by this method with any gas composition.

References

1. C. Yan, D. Xue, J. Phys. Chem. B **110**, 7102 (2006). doi: 10.1021/jp0573821
2. X. Yan, D. Xu, D. Xue, Acta. Mater. **55**, 5747 (2007). doi: 10.1016/j.actamat.2007.06.023
3. S.A. Corr, Y.P. Rakovich, Y.K. Gunko, Nanoscale Res. Lett. **3**, 87 (2008). doi:10.1007/s11671-008-9122-8
4. F.J. Owens, Nanoscale Res. Lett. **2**, 447 (2007)
5. S.K. Srivastava, V.D. Vankar, V. Kumar, V.N. Singh, Nanoscale Res. Lett. **3**, 205 (2008)

6. B.P. Singh, D. Singh, R.B. Mathur, T.L. Dhami, Nanoscale Res. Lett. **3**, 444 (2008). doi:10.1007/s11671-008-9179-4
7. S. Takeda, M. Nakamura, A. Ishii, A. Subagyo, H. Hosoi, K. Sueoka, K. Mukasa, Nanoscale Res. Lett. **2**, 207 (2007). doi:10.1007/s11671-007-9053-9
8. K.F. Fu, Y.P. Sun, J. Nanosci. Nanotechnol. **3**, 351 (2003). doi:10.1166/jnn.2003.225
9. E.T. Mickelson, C.B. Huffman, A.G. Rinzler, R.E. Smalley, R.H. Hauge, J.L. Margrave, Chem. Phys. Lett. **296**, 188 (1998). doi:10.1016/S0009-2614(98)01026-4
10. S. Banerjee, M.G.C. Kahn, S.S. Wong, Chem. Eur. J. **9**, 1899 (2003). doi:10.1002/chem.200204618
11. A.R. Harutyunyan, B.K. Pradhan, J.P. Chang, G.G. Chen, P.C. Eklund, J. Phys. Chem. B **106**, 8671 (2002). doi:10.1021/jp0260301
12. M. Zhang, M. Yudasaka, S. Iijima, J. Phys. Chem. B **108**, 149 (2004). doi:10.1021/jp035850q
13. L. Dumitrescu, N.R. Wilson, J.V. Macpherson, J. Phys. Chem. C **111**, 12944 (2007). doi:10.1021/jp067256x
14. N.I. Kovtyukhova, T.E. Mallouk, L. Pan, E.C. Dickey, J. Am. Chem. Soc. **125**, 9761 (2003). doi:10.1021/ja0344516
15. J. Zhu, M. Yudasaka, M.F. Zhang, S. Iijima, J. Phys. Chem. B **108**, 11317 (2004). doi:10.1021/jp0494032
16. Z.Y. Wu, Y.Y. Xu, X.L. Zhang, G.L. Shen, R.Q. Yu, Talanta **72**, 1336 (2007). doi:10.1016/j.talanta.2007.01.052
17. B. Khare, P. Wilhite, B. Tran, E. Teixeira, K. Fresquez, D.N. Mvondo, C. Bauschlicher, M. Meyyappan, J. Phys. Chem. B **109**, 23466 (2005). doi:10.1021/jp0537254
18. A. Hassanien, M. Tokumoto, P. Umek, D. Vrbanic, M. Mozetic, D. Mihailovic, P. Venturini, S. Pejovnik, Nanotechnology **16**, 278 (2005). doi:10.1088/0957-4484/16/2/017
19. A. Felten, C. Bittencourt, J.J. Pireaux, G. Van Lier, J.C. Charlier, J. Appl. Phys. **98**, 074308 (2005). doi:10.1063/1.2071455
20. R. Ionescu, E.H. Espinosa, E. Sotter, E. Llobet, X. Vilanova, X. Correig, A. Felten, C. Bittencourt, G. Van Lier, J.C. Charlier, J.J. Pireaux, Sens. Actuators B Chem. **113**, 36 (2006). doi:10.1016/j.snb.2005.02.020
21. T. Xu, J.H. Yang, J.W. Liu, Q. Fu, Appl. Surf. Sci. **253**, 8945 (2007). doi:10.1016/j.apsusc.2007.05.028
22. B.N. Khare, P. Wilhite, R.C. Quinn, B. Chen, R.H. Schingler, B. Tran, H. Imanaka, C.R. So, C.W. Bauschlicher, M. Meyyappan, J. Phys. Chem. B **108**, 8166 (2004). doi:10.1021/jp049359q
23. Y.W. Zhu, F.C. Cheong, T. Yu, X.J. Xu, C.T. Lim, J.T.L. Thong, Z.X. Shen, C.K. Ong, Y.J. Liu, A.T.S. Wee, C.H. Sow, Carbon **43**, 395 (2005). doi:10.1016/j.carbon.2004.09.029
24. W.S. Tseng, C.Y. Tseng, P.K. Chuang, A.Y. Lo, C.T. Kuo, J. Phys. Chem. C **112**, 18431 (2008)
25. H. Ago, T. Kugler, F. Cacialli, W.R. Salaneck, M.S.P. Shaffer, A.H. Windle, R.H. Friend, J. Phys. Chem. B **103**, 8116 (1999). doi:10.1021/jp991659y
26. Y. Zhang, S.L. Yuan, W.W. Zhou, J.J. Xu, Y. Li, J. Nanosci. Nanotechnol. **7**, 2366 (2007). doi:10.1166/jnn.2007.412
27. A. Wiltner, C. Linsmeier, Phys. Status Solidi A **201**, 881 (2004). doi:10.1002/pssa.200304362
28. M.M. Shaijumon, A.L.M. Reddy, S. Ramaprabhu, Nanoscale Res. Lett. **2**, 75 (2007). doi:10.1007/s11671-006-9033-5
29. A.C. Dillon, M. Yudasaka, M.S. Dresselhaus, J. Nanosci. Nanotechnol. **4**, 691 (2004). doi:10.1166/jnn.2004.116
30. S.R. Jian, Y.T. Chen, C.F. Wang, H.C. Wen, W.M. Chiu, C.S. Yang, Nanoscale Res. Lett. **3**, 230 (2008)
31. S.K. Pillai, S.S. Ray, M. Moodley, J. Nanosci. Nanotechnol. **7**, 3011 (2007). doi:10.1166/jnn.2007.921
32. Q.F. Liu, W.C. Ren, F. Li, H.T. Cong, H.M. Cheng, J. Phys. Chem. C **111**, 5006 (2007). doi:10.1021/jp068672k